Chapter 2

The L3 Detector at LEP

The L3 detector shown in figure 2.1 is designed to study e^+e^- collisions up to 200 GeV with emphasis on high resolution energy measurements of electrons, photons, muons and jets [12]. The detectors are installed within a 7800 ton magnet providing a 0.5 T field. We have chosen a relatively low field in a large volume to optimize the muon momentum resolution, which improves linearly with the field but quadratically with the track length.

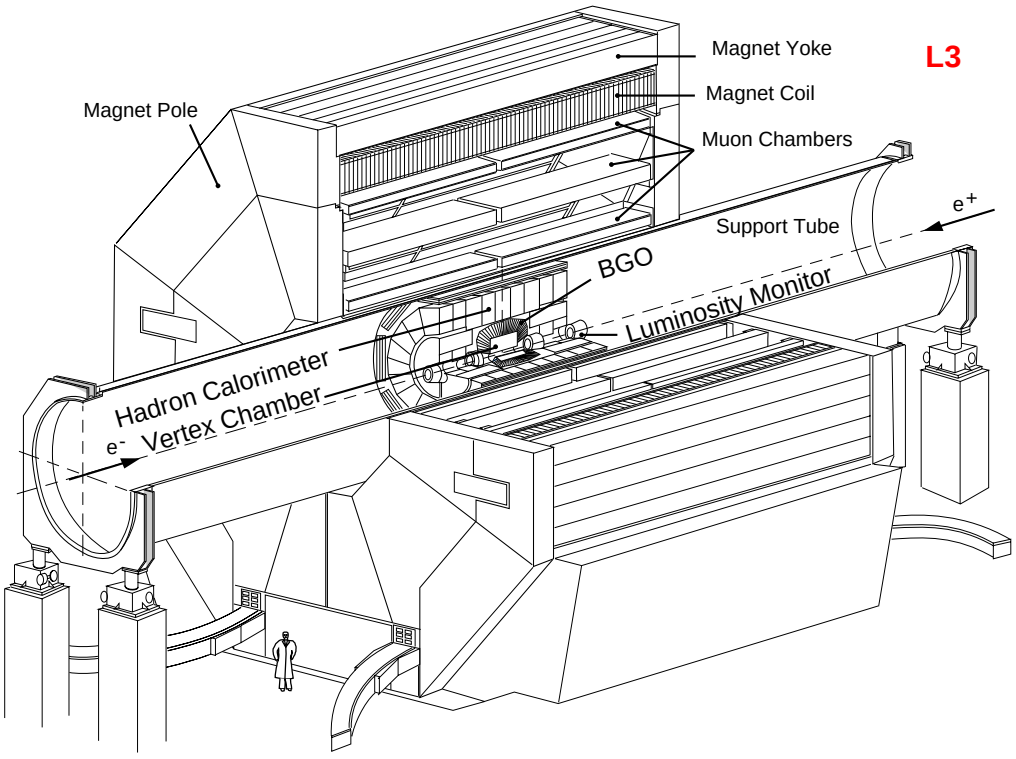

Figure 2.1: The L3 Detector

2.1 General description of the L3 experiment

The detectors are supported by a 32 m long, 4.45 m diameter steel tube. The tube is concentric with the LEP beam line and mechanically coupled to the elements of the low-β insertion, allowing alignment of all L3 detectors relative to the LEP beams. The muon spectrometer forms three concentric chamber layers around the beam, mounted on the outside of the support tube.

The central section of the support tube houses the inner detectors, arranged as "barrel" elements around the beam pipe and as "endcap" elements in the forward and backward directions. The barrel elements consist of muon filter, hadron calorimeter, electromagnetic calorimeter, vertex chamber and the beam pipe. The endcap elements consist of a hadron calorimeter, an electromagnetic calorimeter and a forward tracking chamber. The luminosity monitors are situated immediately in front of the low-β magnets.

2.2 The magnet

The coil (inside radius 5.93 m, total length 11.90 m) is made of aluminum plates welded together. Cooling is provided by two independent circuits made of an aluminum alloy with high resistance to corrosion. The 168 turn coil is divided into 28 packages, each weighing 40 tons, which are bolted together. An active thermal shield placed on the inside of the coil protects the detectors.

The magnetic structure is made of soft iron with 0.5% carbon content. The poles are made of 1100 tons of self-supporting structure giving the required rigidity and serving as a support and reference frame to mount the 5600 tons of filling material, which provides the mass needed for the magnetic flux return, both in the poles and in the barrel. Each pole has two 340 ton half-doors to allow installation and removal of the muon detectors. The magnetic field in the inner volume of the support tube was mapped with Hall probes. The field in the remaining volume has been mapped with about one thousand magnetoresistors, permanently installed on the muon chambers. In addition, five NMR probes monitor the absolute value of the field. The central field in the magnet is 0.5 T.

2.3 The muon detector

The muon detector consists of two ferris wheels, each weighing 86 tons and having eight independent units or octants. Each octant consists of a special mechanical structure supporting five precision (P) drift chambers. There are two chambers (MO) in the outer layer, each with 16 signal wires, two chambers (MM) in the middle layer, each with 24 signal wires, and one inner chamber (MI), with 16 signal wires. They measure track coordinates in the bending plane.

In addition, the top and bottom covers of the MI and MO chambers also consist of drift chambers which measure the z coordinate along the beam. In total there are 6 z-chambers per octant. We used thin aluminum honeycomb with an average of 0.9% of a radiation length per

two layers to enclose the middle chambers. Using this design, a multiple scattering induced sagitta error of less than 30μm at 50 GeV is achieved.

Muons with more than 3 GeV energy are confined to a single octant. Therefore, alignment is only critical between chambers in the same octant. To achieve the design resolution, systematic errors in the internal octant alignment must be kept below 30 μm. The spectrometer covers scattering angles between 36° and 144°.

2.3.1 P- and z-chambers

Each P-chamber contains about 320 signal wires and a total of 3000 wires (including field shaping, cathode and guard wires). The signal and field shaping wires are positioned to about 10 μm in the bending direction and to better than 40 μm in the non-bending direction by precision Pyrex glass and carbon fiber bridges. The chamber cells have been designed to have a very uniform field throughout the active region. An internal alignment system is integrated to the structure of the bridges. This system consists of LED, lenses and quadrant photodiodes. Light from a LED mounted on one end bridge is focused by the lens in the middle bridge onto a quadrant photodiode at the opposite end bridge. The bridges are aligned when all four quadrants of the photodiode receive equal amounts of light. These systems allow us to position the bridges, and thereby the wires, to an accuracy of 10 μm.

The z-chambers consist of two layers of drift cells offset by one half cell with respect to each other to resolve left-right ambiguities. There are in total 96 z-chambers.

The octant stands (Figure 2.2) are precision structures supporting the chambers and maintaining long term chamber alignment to less than 30μm. The structures have been designed to avoid tensor force transmission, thus the octant behavior is fully predictable under all conditions of stress, load and temperature. Special materials, such as titanium and copper-beryllium have been used for chamber support feet, chamber tie-plates, torque-tube joints and other highly stressed areas.

2.3.2 Alignment system and resolution

Opto-mechanical straightness monitors (see figure 2.2) similar to those of the precision bridges are part of the octant alignment system. A precision piece containing two LEDs is attached to each end frame of an inner chamber. A brass pin referenced to the LED touches one wire of a signal plane. The end bridge can be moved so that the wire just makes or breaks its electrical contact to the pin. In this way, the end bridge positions are set to a few μm. The middle and outer chambers have a similar system of pins touching wires. The assembly between the middle chambers contains a lens and that between the outer chambers contains two quadrant diodes. The middle chamber can be moved to bring the chamber centers into a straight line with an error smaller than 10 μm.

The vertical alignment systems guarantee that the chambers line up at each end of the octant, but these two octant center lines must also be parallel to each other. We use a laser

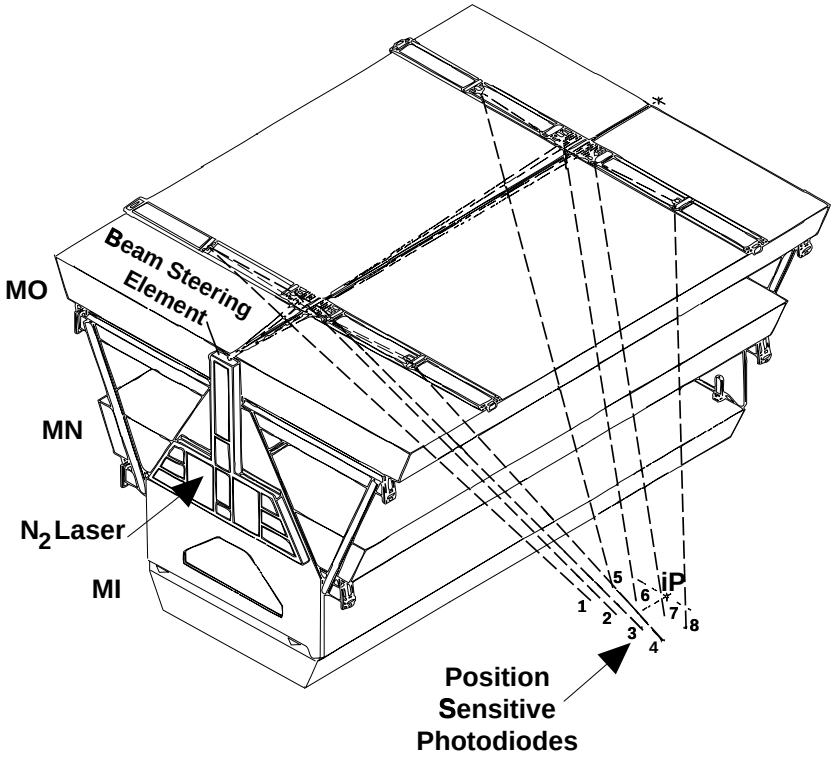

Figure 2.2: A muon chamber octant on its stand

beacon to measure the degree to which the two ends of the octant are parallel. The laser beacon can measure the angle between the two octant center lines to better than 25 μrad, corresponding to an error in the sagitta of less than 10 μm. The MO and MM chambers are adjusted so that this measured angle is zero.

Each of the 16 octants contains a two-stage nitrogen ultraviolet laser. The laser beam is directed up and across the top of the outer chamber layer by an addressable movable beam directional element (Figure 2.2). Mirrors direct the beam down through a quartz window into selected drift cells of all layers of an octant, which are connected by tubes pointing roughly to the interaction point. Photodiodes at the bottom of the MI chamber measure the intensity and position of the beam centroid. Each octant has eight laser beam trajectories, which simulate infinite momentum particles coming from the interaction point. The sagitta of laser events should be zero, and is used to verify the alignment. Two laser beams have movable mirrors and can produce parallel trajectories of exactly known separation, allowing us to measure and constantly monitor the electron drift velocity.

The accuracy of the L3 muon chamber system during the experiment is verified by an analysis of $Z \rightarrow \mu^+\mu^-$ data, taking into account radiative corrections. The result shown in Figure 2.3. The observed resolution of $\sigma(E_{beam}/p_\mu) = 2.5\%$ agrees with the design value.

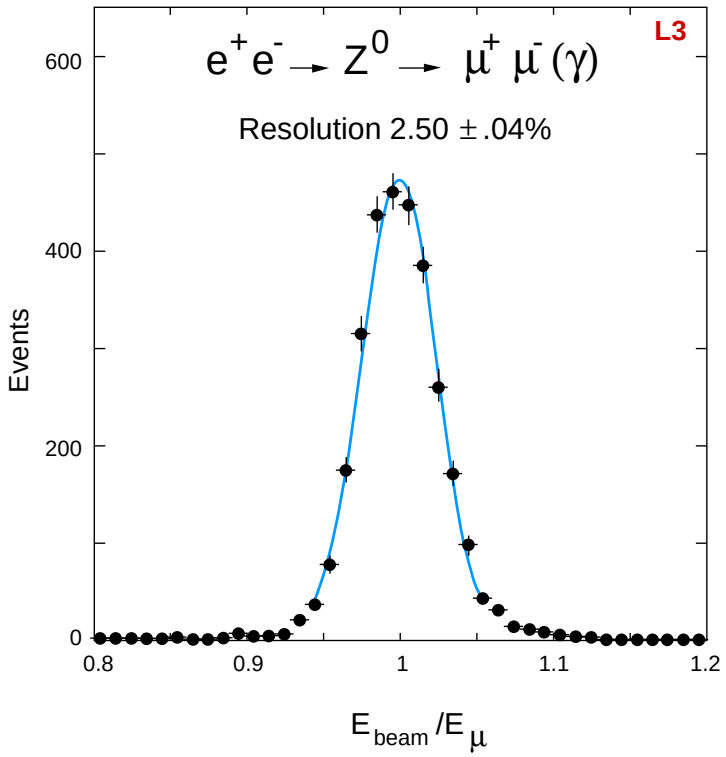

Figure 2.3: The measured momentum resolution of 45 GeV muons in the L3 experiment

2.4 The hadron calorimeter and muon filter

The energy of hadrons emerging from e^+e^- collisions is measured by the total absorption technique with an electromagnetic and a hadron calorimeter. The uranium hadron calorimeter is divided into a barrel part and a forward-backward part. The hadron calorimeter barrel covers the central region ($35° \leq \theta \leq 145°$); it is a fine sampling calorimeter made of depleted uranium absorber plates interspersed with 7968 proportional wire chambers and a total of 370'000 wires; it acts as a filter as well as a calorimeter, allowing only non-showering particles to reach the precision muon detector. The barrel hadron calorimeter has a modular structure consisting of 9 rings of 16 modules each (Figure 2.4).

The wires in each module are grouped to form readout towers. In the ϕ projection the towers point to the beam axis with a constant angular interval. The segmentation is 9 layers in ϕ and z and 10 (8) in the radial direction for the long (short) modules. Typically, a tower covers $\Delta\theta = 2°$, $\Delta\phi = 2°$. The thickness including electromagnetic calorimeter and support structure is at least six nuclear absorption lengths in the barrel part.

The endcaps of the hadron calorimeter cover the polar angle regions $5.5° \leq \theta \leq 35°$ and $145° \leq \theta \leq 174.5°$ over the full azimuthal range, and thus extend the coverage of the hadronic calorimetry to 99.5% of 4π. Each end-cap consists of three separate rings: an outer ring and two inner rings. Each ring is split vertically into half-rings, resulting in a total of 12 separate modules. The modularity of the endcap detectors permits their fast withdrawal to provide access to the other L3 central detector components. The endcaps consist of stainless steel

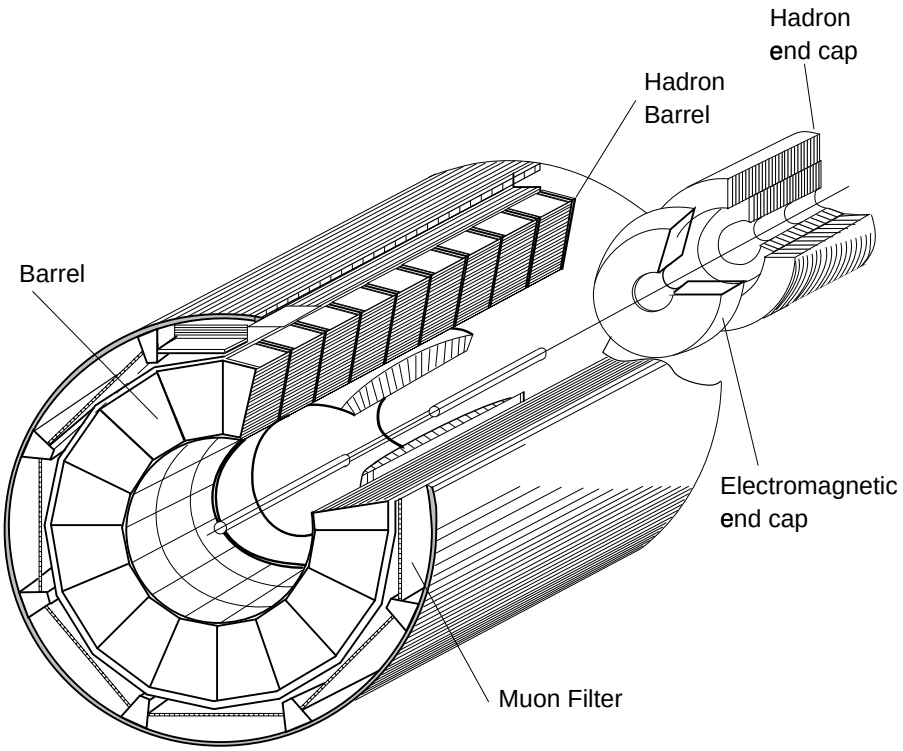

Figure 2.4: The hadron calorimeter

containers filled with alternating layers of brass tube proportional chambers and 5.5 mm thick absorber plates of depleted uranium. The amount of material traversed by a particle originating at the interaction point varies between 6 and 7 nuclear absorption lengths. The wire signals are grouped to form 3960 towers, with $\Delta\theta = 2°$, $\Delta\phi = 2°$.

A muon filter is mounted on the inside wall of the support tube and adds 1.03 absorption lengths to the hadron calorimeter. It consists of eight identical octants, each made of six 1 cm thick brass (65% Cu + 35% Zn) absorber plates, interleaved with five layers of proportional tubes and followed by 1.5 cm thick absorber plates matching the circular shape of the supporting tube.

The energy resolution of the calorimeter in conjunction with the other relevant subdetectors is shown in figure 2.12. The fine segmentation of the calorimeters allows the measurement of the axis of jets with an angular resolution of approximately 2.5°, and of the total energy of hadronic events from Z decay with a resolution of better than 10%.

2.5 The scintillation counters

The scintillation counter system consists of 30 single plastic counters and is located between the electromagnetic and hadronic calorimeters. A polar angle coverage corresponding to $|\cos\theta| < 0.83$ and an azimuthal coverage of 93% is achieved.

The scintillator hit multiplicity is used to trigger hadronic events. The system also records

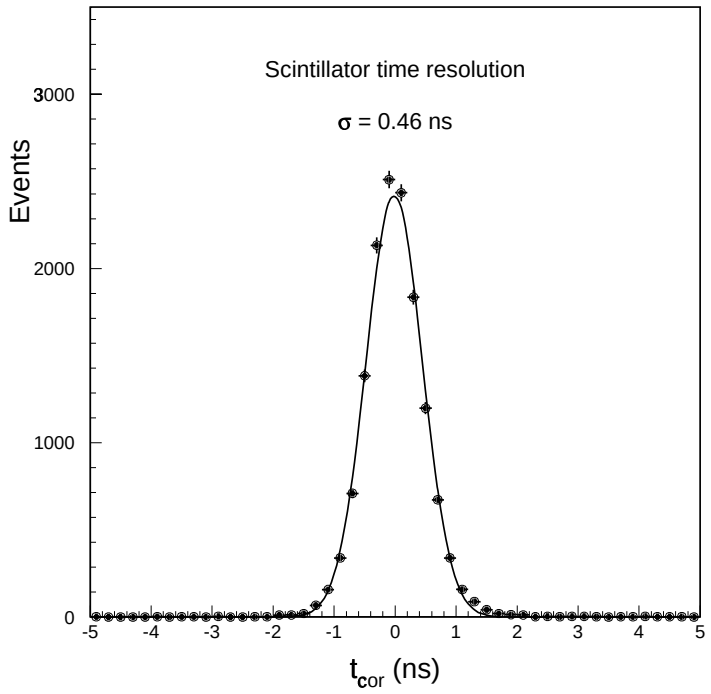

Figure 2.5: Scintillator time corrected for the expected time-of-flight for $e^+e^- \rightarrow \mu^+\mu^-$

the particle's time-of-flight which is used to distinguish dimuon events from cosmic ray background. A single cosmic muon which passes near the interaction point can fake a muon pair event produced in e^+e^- interaction. However, the time difference between opposite scintillation counters is 5.8 ns for cosmic muons and zero for muon pairs. The distribution of the measured time, corrected for the expected time-of-flight (t_{cor}) is shown in figure 2.5 for Z decays into muon pairs. A resolution of 460 ps is achieved.

2.6 The electromagnetic calorimeter

The electromagnetic detector has excellent energy and spatial resolution for photons and electrons over a wide energy range (from 100 MeV to 100 GeV). It uses bismuth germanium oxide (BGO) as both the showering and detecting medium. The electromagnetic calorimeter consists of about 11000 BGO crystals pointing to the interaction region. The detector (see. Figure 2.6) surrounds the central track detector and consists of:

- two half barrels of BGO crystals; the 7680 crystals of the barrel are arranged in two symmetrical half-barrels, giving a polar angle coverage $42° < \theta < 138°$;
- two endcaps, each made of 1527 BGO crystals, with a tracking chamber (FTC) in front, with polar angle coverage $11.6° < \theta < 38°$.

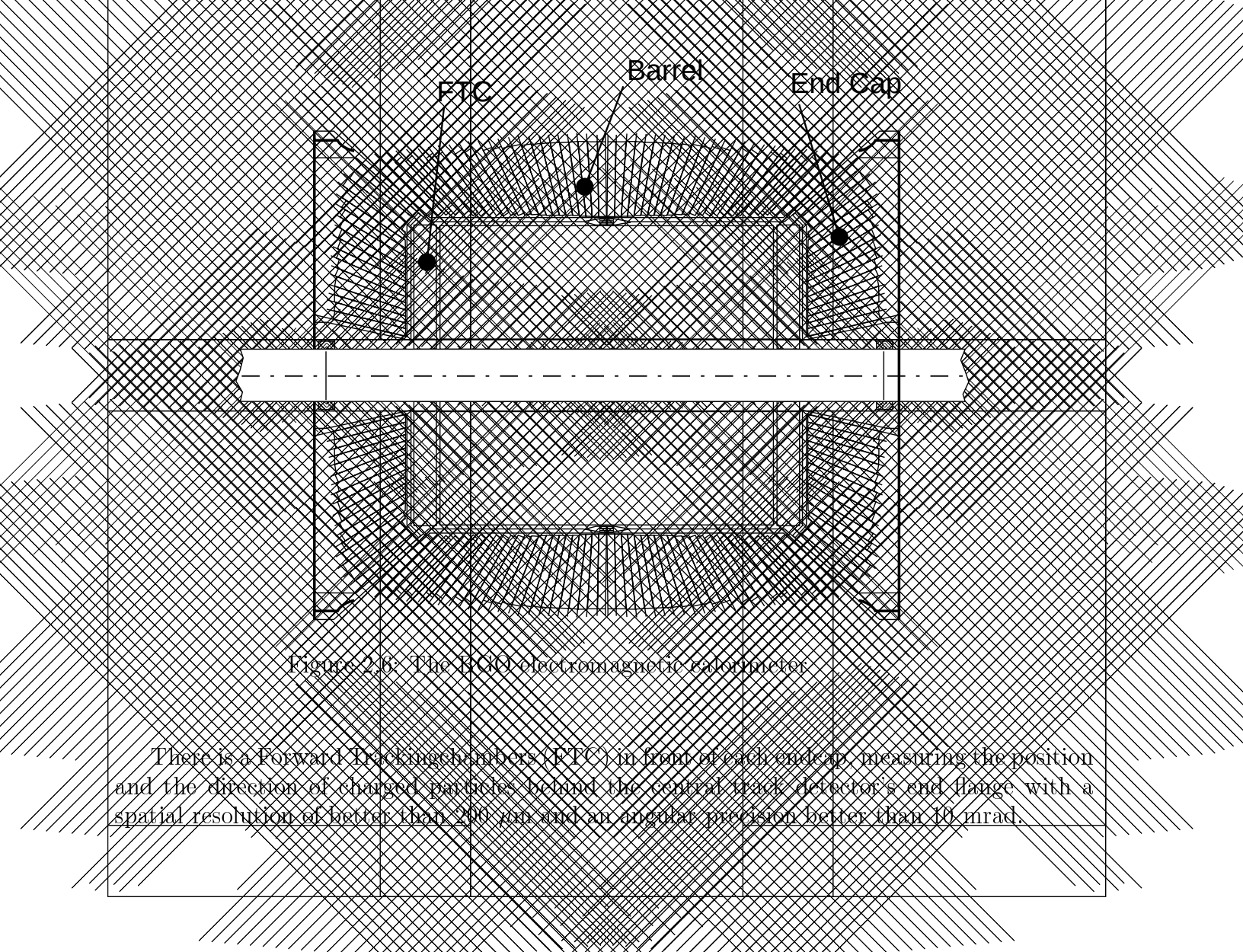

Figure 2.6: The BGO electromagnetic calorimeter

There is a Forward Trackingchambers (FTC) in front of each endcap, measuring the position and the direction of charged particles behind the central track detector's end flange with a spatial resolution of better than 200 μm and an angular precision better than 10 mrad.

2.6.1 BGO crystals and supporting structure

Each BGO crystal is 24 cm long and is a truncated pyramid of about $2 \times 2cm^2$ at the inner end and $3 \times 3cm^2$ at the outer end. All crystals point to the interaction region, with a small angular offset to suppress photon leakage. By coating the polished crystals with a 40 to 50 μm thick layer of high reflectivity paint, one obtains a nearly uniform light collection efficiency.

To achieve the best solid angle coverage and to minimize dead spaces between crystals, the structural material is confined to thin walls around the cells and to a cylindrical inner tube attached on each side to a conical funnel which carries the weight. Each crystal is held in a separate cell with clearances such that normal structural deformation does not affect any crystal and that the weight of a crystal is not transferred to its neighbors. Each crystal is separated from its neighbors by a composite wall, made of two layers of 100 μm pre-impregnated carbon cloth. Cellular walls and clearances represent about 1.75% of the solid angle covered by the barrel.

2.6.2 Readout electronics

Each crystal has two photodiodes glued to its rear face. We use $1.5cm^2$ photodiodes to detect the BGO scintillation light; they are insensitive to the magnetic field and have a quantum efficiency of about 70%. The charge sensitive amplifier is mounted directly behind each crystal. The analog-to-digital converter (ADC) has been designed to satisfy two basic requirements: to measure signals accurately over a wide range, from 10 MeV to 100 GeV and to have a short memory time so that tails from large signals do not mimic small signals in later beam crossings. The digitizing range of the ADC is equivalent to a 21 bit ADC, with a resolution at least 10 bits (i.e. 1000:1) for signals greater than 100 MeV. The linearity is better than 1% over the full range. The actual dynamic range achieved for BGO signals is 20000:1, from full scale to noise level.

2.6.3 Energy calibration and resolution

The barrel part of the calorimeter was calibrated at CERN in an SPS beam, where an accuracy better than 1% was obtained [12]. Sufficient statistical accuracy was achieved by recording about 1600 electrons for each crystal at 2, 10 and 50 GeV momenta. Since one of the most important parameters of the BGO detector is its resolution at low energy, this was tested at a specially designed beam line providing 180 MeV electrons at the LEP injector linac. The energy resolution is $\simeq 5\%$ at 100 MeV and about 1.4% at high energies; the measured spatial resolution above 2 GeV is better than 2 mm and the hadron/electron rejection ratio is about 1000:1. The measured energy resolution for electrons from $Z \rightarrow e^+e^-$ is shown in figure 2.7.

The transparency of the BGO crystals is sensitive to ionizing radiation doses, for instance bursts of X-rays accidentally produced by the LEP beams. A typical beam loss close to the L3 apparatus deposits a few Grays on the inner end cap crystals. At room temperature, the crystals recover their transparency to within 80 to 90% over a few days.

A xenon light monitor [16] measures this transparency by means of light pulses injected into each crystal through a network of optical fibers. It also enables us to track the overall response (except for the scintillation efficiency) of a given crystal relative to its neighbors. The absolute calibration is maintained to within 0.9% by combining the Bhabha scattering information with the xenon monitor information.

In addition, cosmic muons are used to monitor the calibration constants as measured in the test beam and to perform periodic calibration in situ to ensure the stability of the calorimeter's energy response. Figure 2.8 shows reconstructed $\gamma\gamma$ mass spectra from hadronic events at LEP, demonstrating the performance of the electromagnetic calorimeter.

2.7 The central track detector

The total lever arm for coordinate measurement in the central tracking detector is 31.7 cm radially. The charge identification of 50 GeV particles with 95% confidence level requires 50

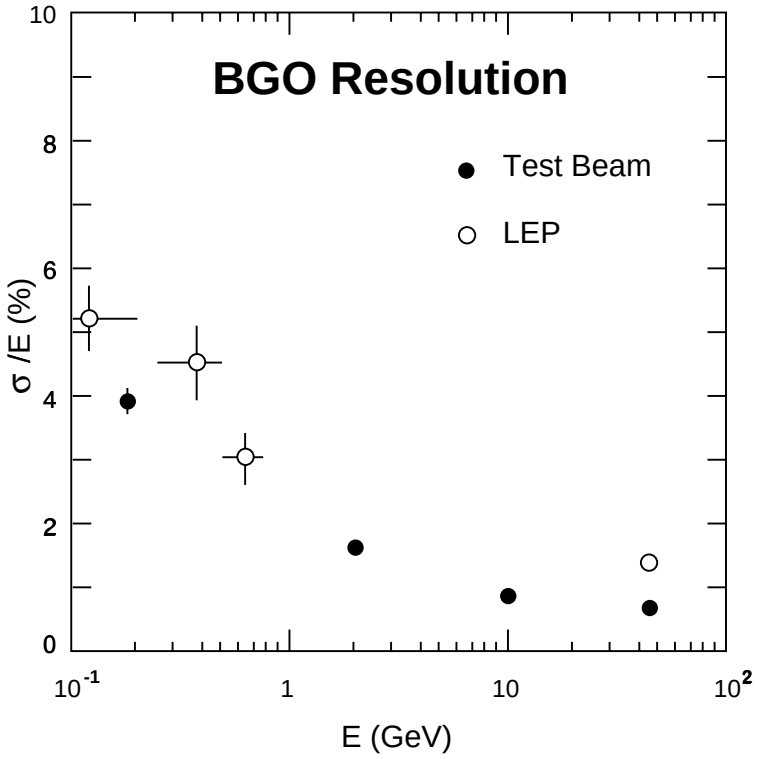

Figure 2.7: The barrel electromagnetic calorimeter energy resolution for electrons as a function of their energy in the L3 experiment.

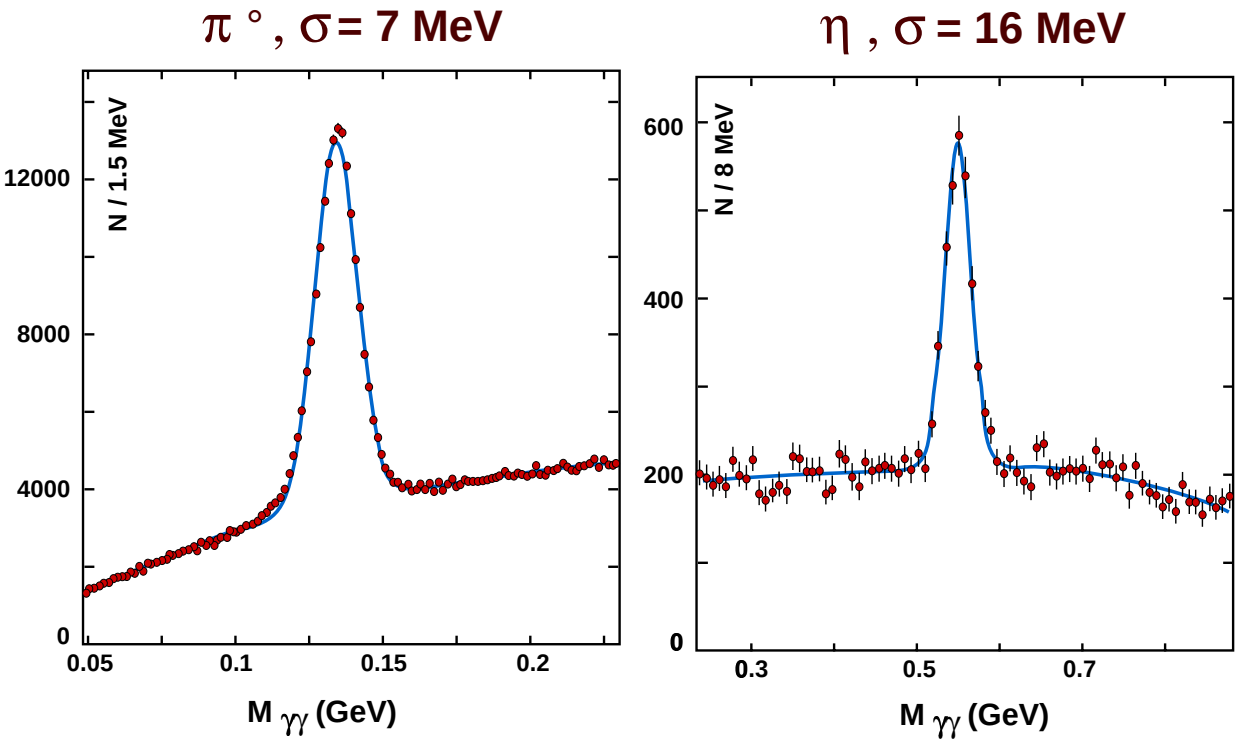

Figure 2.8: Measured $\gamma\gamma$ mass spectra from hadronic events at LEP

coordinate measurements with 50 μm resolution. This is accomplished by a Time Expansion Chamber (TEC), surrounded by two cylindrical proportional chambers with cathode strip

readout, the z-detector (Figure 2.9). Following the TEC principle, the high field amplification region at the sense wire plane is separated from the low field drift region by an additional grid wire plane. This configuration allows to optimize the electron arrival time distribution as well as the track length seen by individual anode wires and choos a drift velocity in the drift region independent of gas amplification constraints. The TEC operates with a low diffusion 80% CO_2 and 20% iC_4H_{10} gas mixture at a pressure of 1.2 bar(abs) and a low drift velocity of 6μm/ns. Furthermore, this gas mixture has a small Lorentz angle of 2.3°. To reach the required resolution, determination of the drift time by a center of gravity method is mandatory. Thus the anode pulses are sampled by Flash Analog to Digital Converters (FADC) after shaping the analog pulses to cancel the ion tail. This principle has been tested by prototype chambers in test beams and in the MARK J experiment at PETRA.

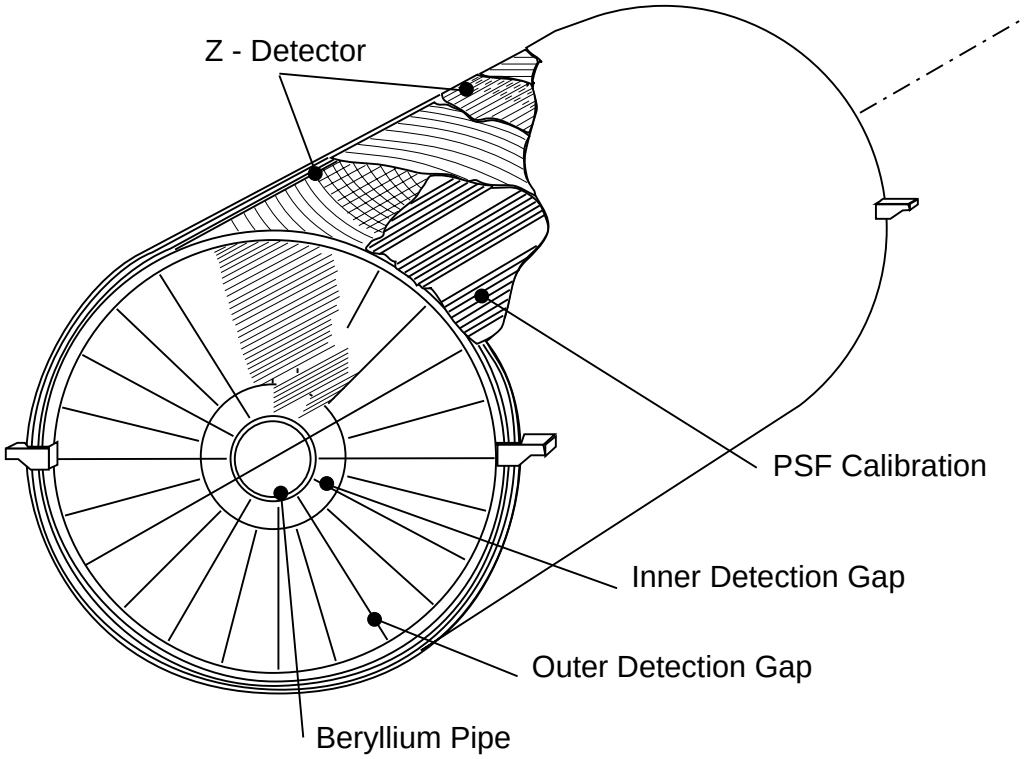

Figure 2.9: The Time Expansion Chamber

The z-detector consists of two thin cylindrical multiwire proportional chambers with cathode strip readout, covering the outer cylinder of the TEC. The cathode strips are inclined with respect to the beam (z-) direction by 69° and 90° for the inner chamber, and by $-69°$ and 90° for the outer chamber.

Each TEC segment is equipped on its outer surface with a plastic scintillation fiber ribbon to monitor the drift velocity to an accuracy of 0.1%. The time-drift distance relationship is obtained for every anode by averaging over the fitted tracks using the e^+e^- interaction point and the fiber position.

Figure 2.10 shows the measured single point resolution of the TEC. The z-detector supplements these $R-\phi$ measurements with z-coordinates just outside the TEC. Its resolution was measured to be 320 μm (see Figure 2.11).

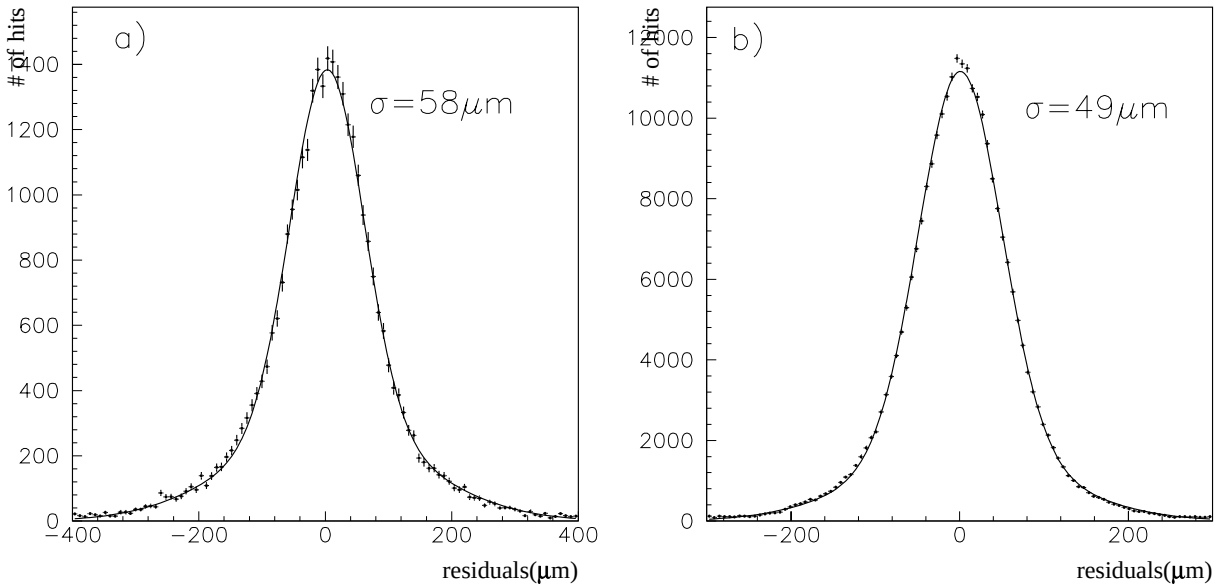

Figure 2.10: Single wire residuals for the TEC chamber in a) the inner and b) the outer ring.

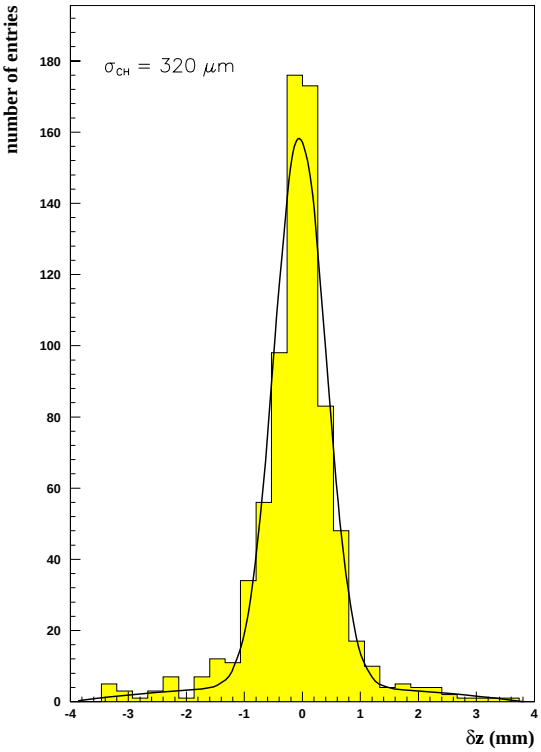

Figure 2.11: The measured z-chamber position resolution

Figure 2.12 shows that the 10.2% resolution of the L3 calorimeters for the total energy of hadronic events improves to 8.4% when the momentum measurement from the central tracking detector is included.

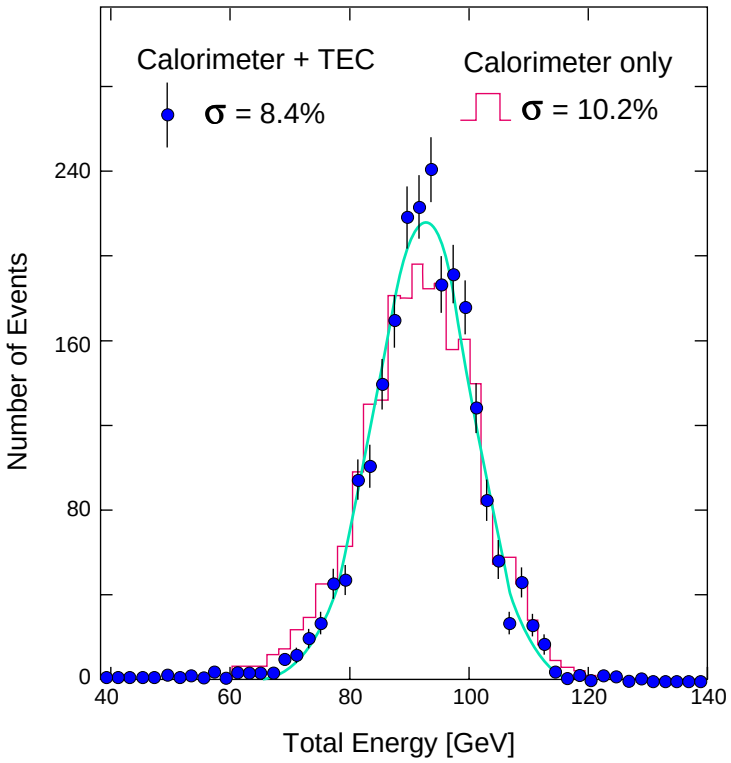

Figure 2.12: The energy resolution for the calorimeters, 10.2%, and its improvement to 8.4% on inclusion of the TEC information

2.8 The luminosity monitor

The luminosity monitor consists of two electromagnetic calorimeters and two sets of proportional wire chambers, situated symmetrically on either side of the interaction point. Each calorimeter is a finely segmented and azimuthally symmetric array of 304 BGO crystals covering the polar angular range $24.93 < \theta < 69.94$ mrad (or $(\pi - \theta)$) (with respect to the interaction point $x = y = z = 0$). Each crystal is read out by a photodiode and has a LED to monitor its stability. The analog photodiode signals are used for the luminosity triggers, and the digitized photodiode signals are used to determine the energy deposited in the crystals. The energy resolution of the calorimeters is about 2% at 45 GeV, and the angular resolution is 0.4 mrad in θ and 0.5° in ϕ.

2.9 The trigger

The overall goal of the L3 trigger system is to record the detector signals from each beam crossing in which particles came from the e^+e^- vertex. By design the only deadtime in the system is incurred during the digitization of the detector signals. This is achieved by a cascade of three digital trigger levels with intermediate buffering. To ensure good efficiency for each physics channel, each level has redundant selection criteria which are logically OR'd to arrive at a decision. To attain the highest precision in the event reconstruction the settings and calibrations of the accelerator, detector and trigger systems are frequently monitored and recorded. The

functions of the three trigger levels are described below. All rates and thresholds noted are "typical".

2.9.1 Level-1 trigger

The level-1 has five triggers based on the calorimeters (electromagnetic and hadronic), luminosity monitors, scintillation counters, muon chambers and the TEC chamber. Each is gated by the beam crossing signal. On a positive result from any of the five, the fine digitization electronics commence operation. On a negative result, all electronics are cleared and readied for the next beam crossing. The level-1 rate of positive decisions is less than 8 Hz, with a dead time incurred from the fine digitizations of less than 5 %.

Calorimeter trigger

The level-1 calorimeter trigger is designed to select events which energy in the electromagnetic or hadronic calorimeters. This includes e^+e^-, $\tau^+\tau^-$, hadronic and $\nu\bar{\nu}\gamma$ final states.

The inputs are the analog sums of several BGO crystals or hadron calorimeter towers. The barrel and endcap BGO crystals are grouped into 32 $\phi\times$ 16 $\theta = 512$ superblocks. The hadron calorimeter is split into 2 radial layers and grouped into 16×11 (16×13) superblocks for the layer less than (greater than) about one absorption length in depth. The signals from a total of 896 channels are digitized and converted into GeV depositions. A series of memory stacks, arithmetic and memory lookup units then calculate several quantities which are compared to preset thresholds. Events with any of these values over threshold are accepted. The quantities used are: the total calorimeter energy; the energy in the electromagnetic calorimeter alone; and these two energies measured only in the barrel region. Typical thresholds are 25, 25, 15 and 8 GeV respectively. In addition θ and ϕ projections are formed to search for clusters, which are accepted with a threshold of 6 GeV. In spatial coincidence with a track from the TEC trigger, this threshold is reduced to 2.5 GeV. These projections are also used to search for events with only a single isolated electromagnetic cluster from single photon events with a threshold of 1 GeV.

The main source of background for this trigger is electronic noise. Typical total rates are 1 to 2 Hz.

Scintillator trigger

Trigger information from the scintillators is used to select high multiplicity events and, as described in the next section, to reject cosmic rays.

To be used as input, the mean time of a hit from any of the 30 scintillators is required to be within a loose gate of 30 ns. The rate of beam crossings with these good hits is about 3 kHz, owing to the proximity of the uranium in the barrel hadron calorimeter. High multiplicity

events are selected by requiring 5 hits spread by over 90°. The rate of this trigger is typically 0.1 Hz and it is practically background free.

Muon trigger

The muon trigger selects events with at least one particle which penetrates the muon chambers.

Each wire in all of the muon chambers is scanned for a signal. Hits are formed if either of a pair of radially adjacent wires shows a signal. These hits are fed through a series of logic units and the event selected if the hits match any possible road from a track with a transverse momentum greater than 1 GeV as measured in either 2 out of 3 of the P-chamber layers or 3 out of 4 of the Z-chambers.

The trigger rate of 10 Hz is dominated by cosmic rays coincident with the beam crossing gate. By requiring in coincidence one good hit from the scintillator trigger this rate is reduced to less than 1 Hz.

TEC trigger

The TEC trigger is used to select events with charged tracks. This includes most of the physics of interest.

The split off signals from 14 anode wires spread radially over each of the outer 24 TEC sectors are used as input. Hits found in these signals are divided into 2 equal drift time bins. Logic units then scan each bin and its adjacent bins looking for tracks while allowing for the θ dependent chamber coverage and efficiency. The minimum transverse momentum selected is 150 MeV. Events are selected if at least two tracks are found with an acolinearity of less than 60°.

The trigger rate is dependent on the beam conditions, varying from 1 to 4 Hz.

Luminosity trigger

The luminosity trigger has as input the analog sums from the luminosity monitor. On each side the monitors are split into 16 ϕ segments and processed as like the calorimeter trigger. Any of three thresholds must be met to accept the event: Two back-to-back (within $\pm$ 1 sector) depositions with $\geq$ 15 GeV, total energy on one side greater than 25 GeV and on the other one greater than 5 GeV, or a total energy in either end greater than 30 GeV. The latter trigger is used to check the efficiency of the previous two and is prescaled by a factor of 20. As the statistical error does not dominate the luminosity determination the first two triggers are prescaled by a factor of two from the 1991 running period onward.

The typical trigger rate of 1.5 Hz depends primarily on the delivered luminosity but can increase in especially bad background conditions.

2.9.2 Level-2 trigger

The level-1 triggers attempt to select interesting events. In contrast, the function of the level-2 trigger is to reject background events selected by level-1. The input to the level-2 trigger are the coarse data used in level-1, the level-1 results and a few more data available for analysis at this step. The improvement on the level-1 results derives from the ability of level-2 to spend more time per event without incurring additional deadtime and on its ability to correlate subdetectors signals. This is especially effective in removing calorimeter triggers generated by electronic noise and TEC triggers generated by beam-gas, beam-wall interactions as well as synchrotron radiation. On a positive or negative result the level-2 results and all input is forwarded to an event builder memory. Other memories contain the zero suppressed fine digitizations from each subdetector. On a positive level-2 result the event builder collates the data for the entire event and transfers it to the level-3 trigger. On a negative level-2 result the event builder memories are reset. Events that fulfill more than one level-1 trigger condition pass the level-2 unhindered. The rejection power is typically 20 to 30% averaged over all level-1 triggers, such that the total rate after of level-2 is typically less than 6 Hz.

2.9.3 Level-3 trigger

To be effective level-3 applies criteria based on the complete digital data for the event. Several algorithms are used to examine the event, with the specific algorithm used being driven by the level-1 trigger which selected the event (calorimeter, luminosity, muon or TEC). As for level-2, events which were selected by more than one trigger at level-1 pass through unhindered. The calorimeter algorithm recalculates the event energies and applies similar criteria to those of the calorimeter trigger to pass the event. As the calculations are based on the fine digitizations the thresholds can be more precisely defined and electronic noise problems are further reduced. Luminosity triggers are passed through untouched. Muon triggers are required to pass a more stringent scintillator coincidence in time, $\pm$10ns, and space, $\pm 60^\circ$. Tracks from TEC trigger events are correlated with at least 100 MeV of energy in the calorimeters and also examined for quality and a common vertex. Taken together these algorithms result in a rate reduction of 40 to 60%, with an output rate of 2 to 3 Hz.

The output from the level-3 trigger is delivered into a memory buffer on the main online computer. From this buffer all events are written to tape and selected events dispatched to ten separate monitoring programs. In addition, processes on this and the other online computers control the data taking, monitor, log and adjust detector settings, and calibrate the various detector and trigger elements.

2.10 The LEP collider complex

The Large Electron Positron collider LEP at CERN is situated in a tunnel of 27 km circumference on both sides of the border between France and Switzerland (see figure 2.13).

The main components of the collider are

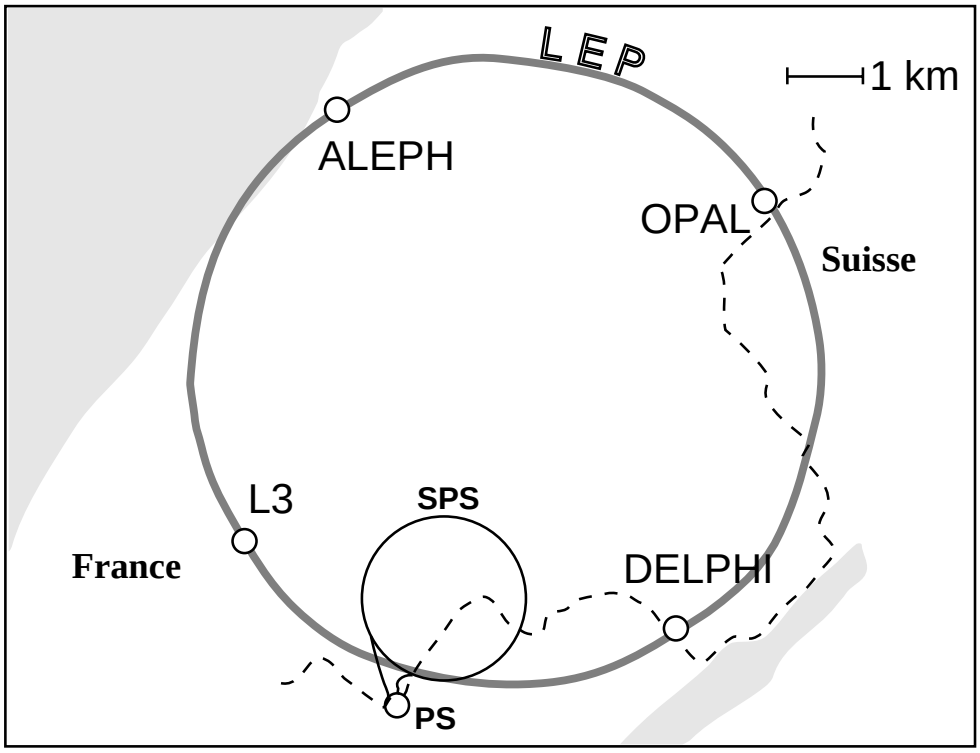

Figure 2.13: The LEP collider at CERN

- eight bending sections of 2840 m length each, with in total 3304 dipole magnets. At 45 GeV beam energy, the required field is 0.048 T.
- eight straight sections, four of which house the experiments ALEPH [10], DELPHI [11], L3 [12] and OPAL [13]. To both sides of each experiment, the beam is compressed with superconducting quadrupole magnets, increasing the luminosity.
- two straight sections containing the radiofrequency cavities with a total power of 16 MW, to accelerate the beam from injection energy to collision energy and to replace the energy lost by radiation on each turn.
- the existing accelerators PS and SPS, which are used as part of the injection system in addition to the linear accelerator LIL and an accumulation ring to enhance positron intensity.

At the beginning of each LEP fill, positrons and electrons are injected at an energy of 20 GeV. After ramping to collision energies, the beam lifetime is usually of the order of 20 hours at typical currents of up to 0.5 mA. The typical instantaneous luminosity delivered to L3 in 4×4 bunch operation during the later part of 1991 was $3 \times 10^{30}\mathrm{cm}^{-2}\mathrm{s}^{-1}$, with peak values reaching $5 \times 10^{30}\mathrm{cm}^{-2}\mathrm{s}^{-1}$.

In agreement with the originally proposed schedule of LEP, the collider has so far been run at energies at and around the Z resonance. Figure 2.14 shows the history of integrated luminosity delivered to the L3 experiment as a function of time. It is seen that in a short period after its commissioning, substantial improvements in luminosity have been achieved.

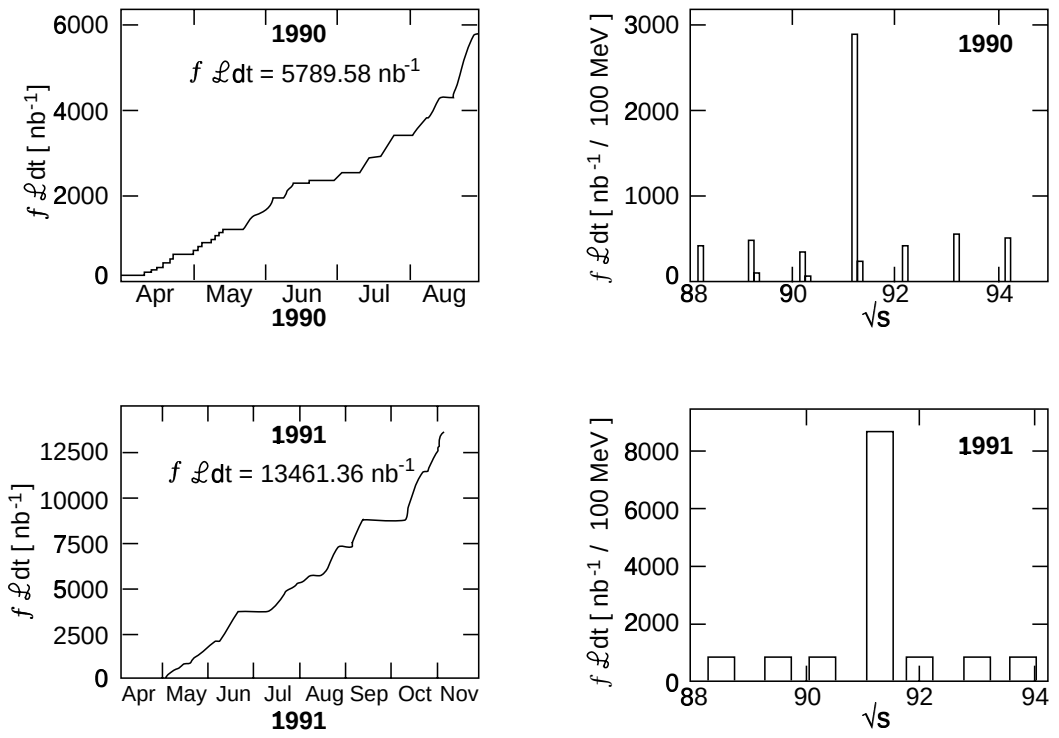

Figure 2.14: The history of integrated luminosity delivered to L3 in 1990 and 1991.

2.11 LEP collider energy calibration

The energy calibration of LEP is described in reference 17. The mass of the Z boson is a fundamental parameter of the Standard Model and its systematic error is dominated by the uncertainties in the LEP beam energies. Accordingly, four different methods have been used to provide information on the energy and to enable cross-checks to be made:

1. *The Field Display* uses a rotating coil to measure the magnetic field in reference dipoles powered in series with the main ring magnets. The reproducibility of the field display measurements is about 2.5×10^{-5}.

2. *The Flux Loop* consists of a closed electrical loop threading through all the dipoles; the integrated induced voltage when altering the dipole currents is a direct measure of the magnetic field generated by the main ring dipoles. However, it is insensitive to constant fields and does not take into account additional bending due to the quadrupoles and sextapoles on non-central orbits. Its absolute calibration has a precision of about 10^{-4}, but the additional corrections required reduce this precision.

3. *Proton Calibrations* are performed by filling the ring with 20 GeV protons which are not ultra-relativistic and thus their momentum can be measured by determination of the frequency of the RF acceleration voltage, this determines the momentum of positrons in a similar orbit. The precision of this method is high at 20 GeV but degrades to 2×10^{-4} after extrapolation to 45 GeV.

4. *Resonant Depolarization* determines the beam energy by measuring the frequency with which the spins of transversly polarized electrons precess around the vertical axis. This technique measures the beam energy under conditions very close to those of data-taking runs and is by far the most precise technique available.

In 1991 the absolute energy scale has been determined with a relative precision of 5.7×10^{-5} corresponding to ± 5.3 MeV at a center-of-mass energy of 93 GeV. In addition to the overall scale error, uncertainties in the local energy scale about the normalization point and in the fill-to-fill reproducibility of the beam energy lead to a total error due to energy uncertainties of ± 6.3 MeV on m_{Z}.